SEBHA UNIVERSITY CONFERENCE PROCEEDINGS, VOL.04 NO. 1 2025
DOI: 10.51984/SUCP.V4I1.3933

المؤتمر العلمي الأول للتطبيقات الهندسية (ICEA'2024)
The First Scientific Conference on Engineering Applications (ICEA'2024)
Conference homepage: www.icea.ly

Scrutinization of the Thermal and Aerodynamic Effects of Air Gap Width on Trombe Walls via Computational Fluid Dynamics Simulation

* Omar A. Ibsheesh , Monder O.Albeshty , Giamal Mashina , Akram A.Mousay , Nawal A.Almeesawi , Abraheem A.Sallam

Department of Mechanical Engineering and Energies Libyan Academy for Postgraduate Studies Tripoli, Libya

Keywords:
Trombe Wall
Renewable Energy Sources
Solar Energy
Passive Solar Heating
Sustainable Architecture

ABSTRACT

The Trombe Wall is a venerated passive-solar architectural feature, and it is a key integral to an energy-efficient construction design that functions on a friendly environmental energy source, which is solar energy. This study contemplates and delves into the convoluted interplay between air gap widths within Trombe walls and their influence on room temperature modulation and air dynamics. A comparison of diverse air gap widths of 13mm, 25mm, 34mm, 50mm, and 80mm is conducted, and an investigation of the heat transfer mechanisms and convective flow behavior is performed by utilizing computational fluid dynamics (CFD) simulations. The results illuminate optimal air gap dimensions and equip architects and engineers with imperative understandings for enhancing Trombe walls and passive heating and cooling systems in sustainable building projects.

دراسة التأثيرات الحرارية والديناميكية الهوائية لعرض الفجوة الهوائية في جدران ترومب باستخدام محاكاة ديناميكا السوائل الحسابية

*عمر بشيش و منذر أسامة البشتي و جمال ماشية و اكرم علي موسى و نوال عبد السلام الميساوي و إبراهيم سلام

قسم الهندسة الميكانيكية والطاقات المتجددة، ليبيا

الكلمات المفتاحية:
جدار ترومب
مصادر الطاقة المتجددة
الطاقة الشمسية
التدفئة الشمسية السلبية
العمارة المستدام

الملخص:

تُعتبر جدار ترومب إحدى العناصر المرموقة في تصميمات الهندسة المعمارية الشمسية السلبية، وهو عنصر أساسي في تصميم المباني ذات الكفاءة العالية في استهلاك الطاقة، حيث يعتمد على مصدر طاقة صديق للبيئة وهو الطاقة الشمسية. تتناول هذه الدراسة العلاقة المعقدة بين عرض الفجوات الهوائية داخل جدران ترومب وتأثيرها على تعديل درجة حرارة الغرف وديناميكيات الهواء. تم إجراء مقارنة بين عروض فجوات هوائية مختلفة تشمل 13 ملم، 25 ملم، 34 ملم، 50 ملم، و80 ملم، وتم دراسة آليات انتقال الحرارة وسلوك التدفق الحراري باستخدام محاكاة ديناميكا السوائل الحسابية (CFD). تُظهر النتائج الأبعاد المثلى للفجوات الهوائية وتزود المعماريين والمهندسين بفهم أساسي لتحسين جدران ترومب وأنظمة التدفئة والتبريد السلبية في مشاريع البناء المستدامة.

INTRODUCTION

In a world fueled by wealth and energy, these two elements determine our existence and survival for the coming generations. The energy demands are growing, along with significant environmental crises, so seeking clean and sustainable energy sources is essential. As a result, numerous governments have launched research programs addressing this global challenge. Renewable energy sources such as solar energy present tremendous potential in various engineering fields, particularly heating and cooling systems that maintain comfortable temperatures throughout the year. Implementing these systems not only efficiently utilizes natural energy, but also provides significant environmental benefits, positively influencing all forms of life on Earth.

A Trombe wall (TW) is a passive heating and cooling system strategy that utilizes the sun to provide cozy temperatures. This wall is enclosed from the outside, forming a gap in between for air circulation. The glass permits sunlight to strike the mass wall, delivering heat and warmth during the day. Also, the wall has a high capacity to hold heat energy for usage during the evening and at night.

The TW framework was first developed by Edward Morse in **1881** [1] and was revitalized by Felix Trombe [2]. The materials that construct the TW must have an excellent capacity for heat, such as cement. Sun rays are directed toward the wall, heating it and warming the air by natural convection, making the air rise and circulate in and out of the Air gap. Heat can then be transferred to the room via air

*Corresponding author:
E-mail addresses: omaromy1994@gmail.com, (M. O.Albeshty) monderalbeshty@gmail.com, (G. Mashina) gaimal.mashina@acamedy.edu.ly , (A. A.Mousay) akram.mossa.ak90@gmail.com, (N. A.Almeesawi) itnawalit94@gmail.com, (A. A.Sallam) ibrahemsallam19@gmail.com
Article History : Received 13 March 2024 - Received in revised form 25 September 2024 - Accepted 15 October 2024

circulation through the openings in the wall, which warms the room to a desirable temperature [2].

A study is performed to investigate the temperature distribution across three TW models. The first model is an unvented TW, the second contains vents for winter heating, and the third has vents for summer cooling. It utilized computational fluid dynamics (CFD) simulation software to simulate the energy dynamics and visualize the temperature distribution of these models. The findings revealed that the second and third models consistently exhibited higher temperatures than the unvented TW [3].

On the other hand, TW efficiency has also been studied experimentally based on air gap width variations in the structure of size $(\mathbf{1.5 \times 1 \times 1.5})\ \boldsymbol{m}$, which indicated that the $\mathbf{15}\ \boldsymbol{cm}$ air gap has the highest thermal efficiency among the chosen widths. Empirical equations for instantaneous efficiency are obtained for different air gap widths [4]. Another paper examined the optimal air gap thickness of $\mathbf{1}$, $\mathbf{3}$, and $\mathbf{4}\ \boldsymbol{cm}$, showing an air gap thickness of $\mathbf{1}\ \boldsymbol{cm}$ has more acceptable room heat distribution and air movements than other selected gaps [5].

The forthcoming study investigates the connection between the air gap width of small dimensions in TWs and its implications for thermal distribution and aerodynamics. Notably, the research encompasses a comparative analysis of diverse air gap widths—particularly $\mathbf{13}\ \boldsymbol{mm}$, $\mathbf{25}\ \boldsymbol{mm}$, $\mathbf{34}\ \boldsymbol{mm}$, $\mathbf{50}\ \boldsymbol{mm}$, and $\mathbf{80}\ \boldsymbol{mm}$. The study strives to explain heat transfer mechanisms and convective behavior through two dimensional (2D) CFD simulations.

SIMULATION

Structure geometry

The simulated system inherits the features of conventional TW, it consists of 2D structure measures $(\mathbf{2940 \times 2070})\ \boldsymbol{mm}$, and the boundary of the structure is made of concrete with a thickness of $\mathbf{70}\ \boldsymbol{mm}$ encloses all sides besides the left side, which is created of $\mathbf{5}\ \boldsymbol{mm}$ thick glass with a height of $\mathbf{2870}\ \boldsymbol{mm}$. The mass wall measuring dimensions are $(\mathbf{2800 \times 250})\ \boldsymbol{mm}$ and constructed from cement, positioned away from the glass forming an air gap with a supervised width as desirable during the current study. Furthermore, it features two openings: an Upper Opening and a Lower Opening, with a height of $\mathbf{80}\ \boldsymbol{mm}$ permitting the air circulation from in and out of the air gap.

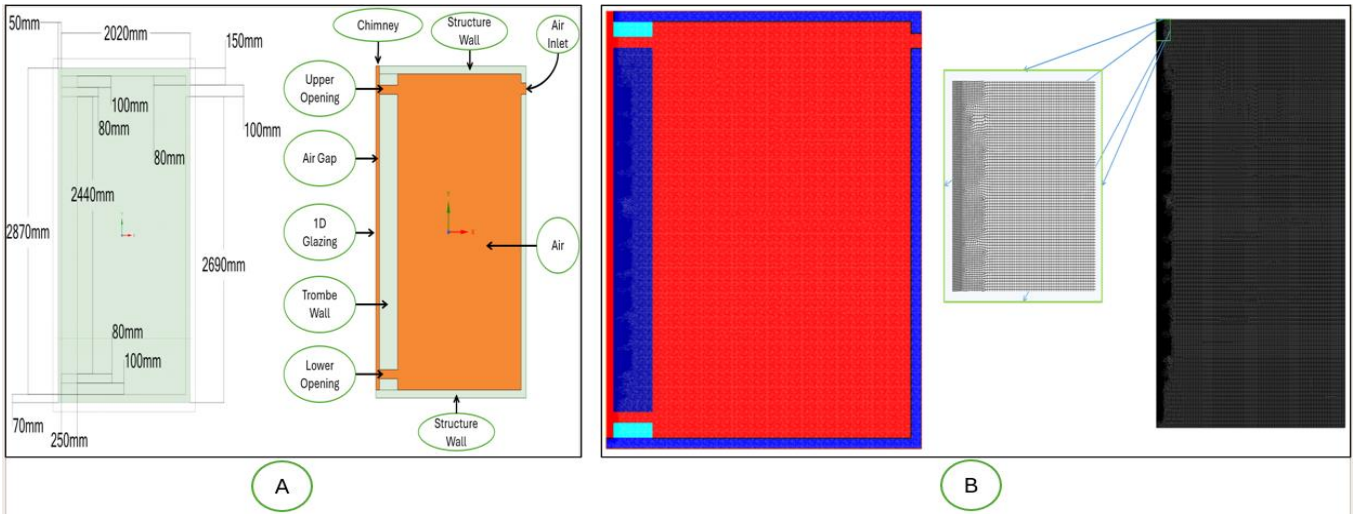

Appendix A. *Figure 1. (A) Structure 2D Design (B) Mesh*

Meshing process

The mesh selection process is a necessary stage for the completion of the simulation, it plays a critical function in retaining accurate results that impact the entirety of CFD simulation. A simple mesh is utilized as the selected structure has non-complicated geometrical regions that yield satisfactory results with less simulation time. Particularly, a uniform mesh of $\mathbf{10}\boldsymbol{mm}$ element size was applied to confine the totality of the domain, specifying a finer meshing procedure with an element size of $\mathbf{5}\boldsymbol{mm}$ in the air gap region, which permits an adequately thorough illustration of the air dynamics within that specific region. The meshing selection is chosen to satisfy the following criteria:

Appendix B. *Table 1. Meshing Criteria*

Criteria	Min Value	Max Value	Average Value	Recommended Values
Skewness (S)	1.3057e-10	0.63469	1.1536e-2	S < 0.85
Aspect Ratio (AR)	1	2.4848	1.0436	1 < AR < 5
Orthogonal Quality (OQ)	0.63564	1	0.99865	OQ = 1
Element Quality (EQ)	0.36192	0.99971	0.98518	EQ = 1

Simulation parameters

The simulation process is conducted for five different widths of air gap and subjected to identical conditions corresponding to the trial widths of $\mathbf{13}\ \boldsymbol{mm}, \mathbf{25}\ \boldsymbol{mm}, \mathbf{34}\ \boldsymbol{mm}$, $\mathbf{50}\ \boldsymbol{mm}, \boldsymbol{and}\ \mathbf{80}\ \boldsymbol{mm}$.

Appendix C. *Table 2. Material Properties*

Material	Density kg/m^3	Specific Heat J/ (kg K)	Thermal Conductivity W/ (m K)
Air	incompressible ideal gas	1006.43	0.0242
Glass soda lime (common glass)	2464.9	898.61	1.0073
Concrete	2391.7	936.35	2.0712
Cement	1990	839.57	0.84853

The boundary conditions are identical for all simulations. As pictured in Figure 1, the structure wall is created from concrete, having an internal emissivity and a diffuse fraction of $\mathbf{0.85}$ and $\mathbf{0.5}$ respectively. A convective thermal boundary condition is applied at the structure externally with a free stream temperature of $\mathbf{10°}\boldsymbol{C}$ and a convective heat transfer coefficient of $\mathbf{10}\ \boldsymbol{W/(m\text{^}2\ K)}$. The structure contains four openings - an Air Inlet and a Chimney, which are both locked with glass windows and conditioned with the exact convective thermal boundary conditions of the structure wall. The Upper and Lower Openings are opened to facilitate the circulation of air and emulate the heating cycle in the Winter season.

The glazing boundary is crafted from soda-lime glass, and it has a mixed boundary conditions of radiation and convection. The convection conditions correspond with those of the structure wall. As for radiation, it is conditioned with an external radiation temperature of $\mathbf{30°}\boldsymbol{C}$, an external emissivity of $\mathbf{0.85}$, and a diffuse fraction of $\mathbf{0.5}$. Solar rays are applied parallel to the horizontal axis perpendicular to the glass, penetrating it into the mass wall. Direct irradiation measures $\mathbf{1000}\boldsymbol{W/m\text{^}2}$, while the diffuse irradiation has a value of $\mathbf{200}\boldsymbol{W/m\text{^}2}$.

The chosen model for simulation is energy, a laminar and discrete ordinate model with an initial domain temperature of $\mathbf{10°}\boldsymbol{C}$, also the simulation is performed in a transient mode with first-order implicit

consisting of **5000**-time steps for **100** Iterations for each step with a time step size of $5s$. The following solver settings are chosen according to trial simulations that conducted prior to the actual simulation, confirming the solution stability and convergence:

Appendix D. *Table 3. Solving Settings*

	Under-Relaxation Factors	Discretization Scheme
Pressure	0.4	Second Order
Density	0.4	/
Body Forces	0.6	/
Momentum	0.4	Second Order Upwind
Energy	0.8	Second Order Upwind
Discrete Ordinates	0.8	First Order Upwind

Mathematical Model

The Trombe Wall system can be simulated by solving numerically the following equations [6]:

Energy Equation:

$$\frac{\partial(\rho E)}{\partial t} + \nabla \cdot \left(\vec{V}(\rho E + p)\right) = \nabla \cdot \left(k \nabla T + \left(\bar{\tau} \cdot \vec{V}\right)\right) + \dot{S}_g$$

Mass Conservation Equation:

$$\frac{\partial \rho}{\partial t} + \nabla \cdot (\rho \vec{V}) = S_m$$

Momentum Conservation Equations:

$$\frac{\partial(\rho \vec{V})}{\partial t} + \nabla \cdot (\rho \vec{V}\vec{V}) = -\nabla p + \nabla \cdot (\bar{\bar{\tau}}) + \rho \vec{g} + \vec{F}$$

The DO Model Equations

$$\nabla \cdot \left(I_{(\vec{r},\vec{s})}\vec{s}\right) + (a + \sigma_s) I_{(\vec{r},\vec{s})} = an^2 \frac{\sigma T^4}{\pi} + \frac{\sigma_2}{4\pi} \int_0^{4\pi} I_{(\vec{r},\vec{s}')}\, \Phi(\vec{s} \cdot \vec{s}')\, d\Omega'$$

Results and Discussions

The simulations provide, as illustrated in the contours, a profound understanding and a comprehensive visual representation of essential parameters such as pressure, air velocity, air mass rate, and temperature. The pressure contour portrayed crosses the distinct widths of the air gap forming low-pressure regions in the air gap at the middle of a mass wall, indicating a uniform static pressure difference of approximately $0.4\,Pa$, with distinct upper and lower bounds pressure values for each system. The rising air of low density can be observed from the density contour, noting that it is closer to the mass wall than the glass as portrayed clearly in the 8cm Air Gap Width density contour, reaching towards the center of the air gap as the width lessens. Likewise, the air dynamics are indicated in velocity and stream contours, exhibiting the formation of minor vortices in a wider air gap generated by the downward motion of cool air adjacent to the glass as opposed to warm air, which can be seen more clearly in the figure of the velocity vector.

The graphs reveal the temperature distribution and air velocity profile across diverse air gap widths in three different regions, namely the middle region, the upper opening region, and lastly the lower opening region. The comparative of temperature and velocity between different air gap widths directly by length illustrates a non-clear understanding comparable to expressing the length by percentage, describing the width of air gap by percentage as 0% is $0\,m$ and 100% is the simulated width of air gap from the mass wall, being 100% of length is the glass cover.

Examination of Figure **7** illustrates the temperature distribution and air dynamics within the middle region. The temperature distribution features a seemingly linear regression at a width of $1.3\,cm$ along the air gap, excluding the few layers above the lower opening, where a non-linear behavior is observed due to the consequence of cool air entering the air gap. As the air gap widens, the formerly linear temperature behavior transforms into a non-linear, resulting in a region within the middle of the air gap that carries an approximately constant temperature relative to the air gap width. Notably, when the air gap width exceeds $3.4\,cm$, the temperature within this region stays constant along the X-axis. It is followed that the temperature within this region increases with height due to the warm air dominating over the cool air. The peak temperature is noted at the highest point of the mass wall at the air gap, although the lowest temperature is noted slightly above the lower opening due to the inflow of cool air.

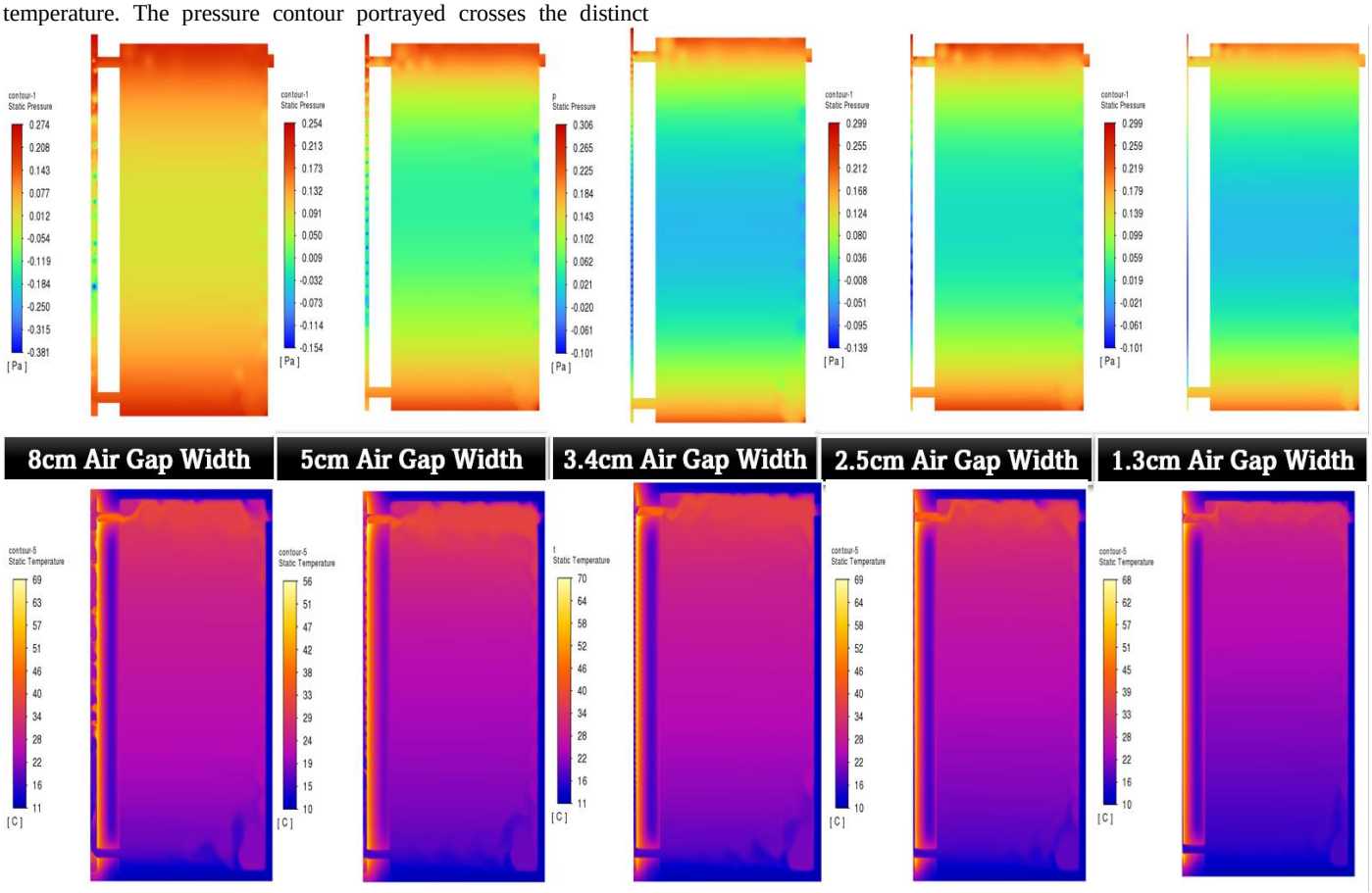

Appendix E. *Figure 2. Pressure and Temperature Contours*

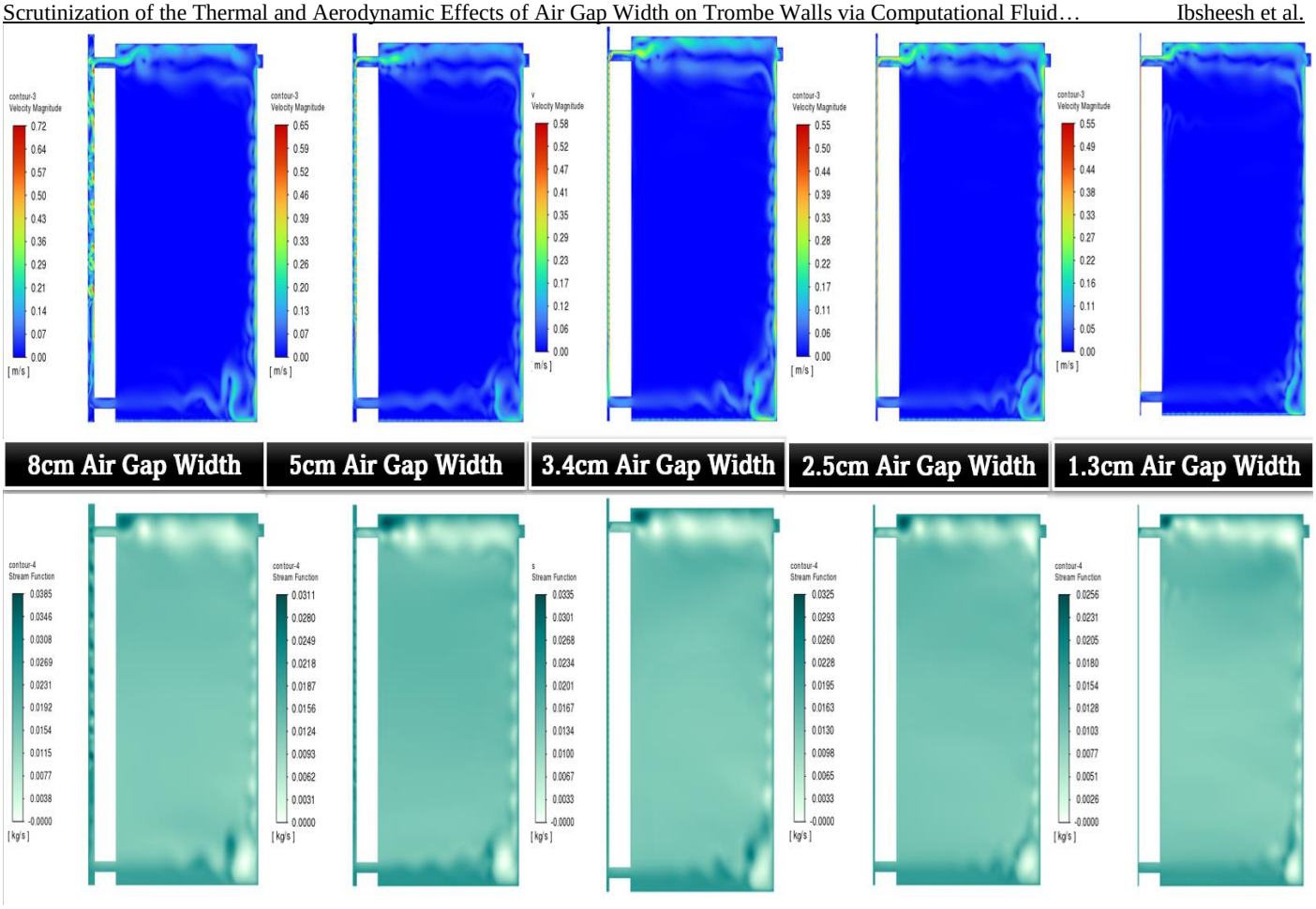

Appendix F. *Figure 3. Velocity and Mass Flow Rate Contours*

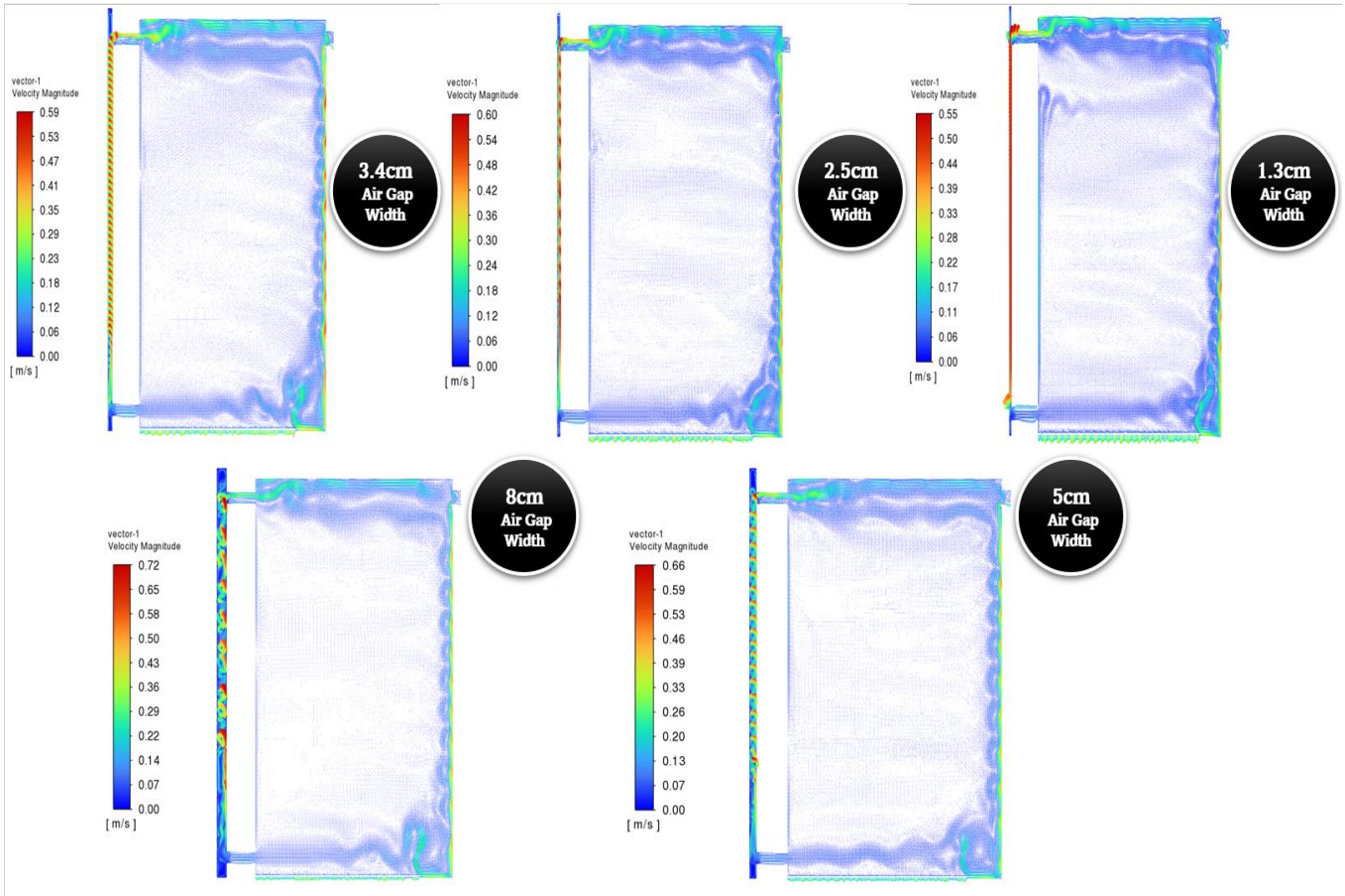

Appendix G. *Figure 4. Air Velocity Vectors*

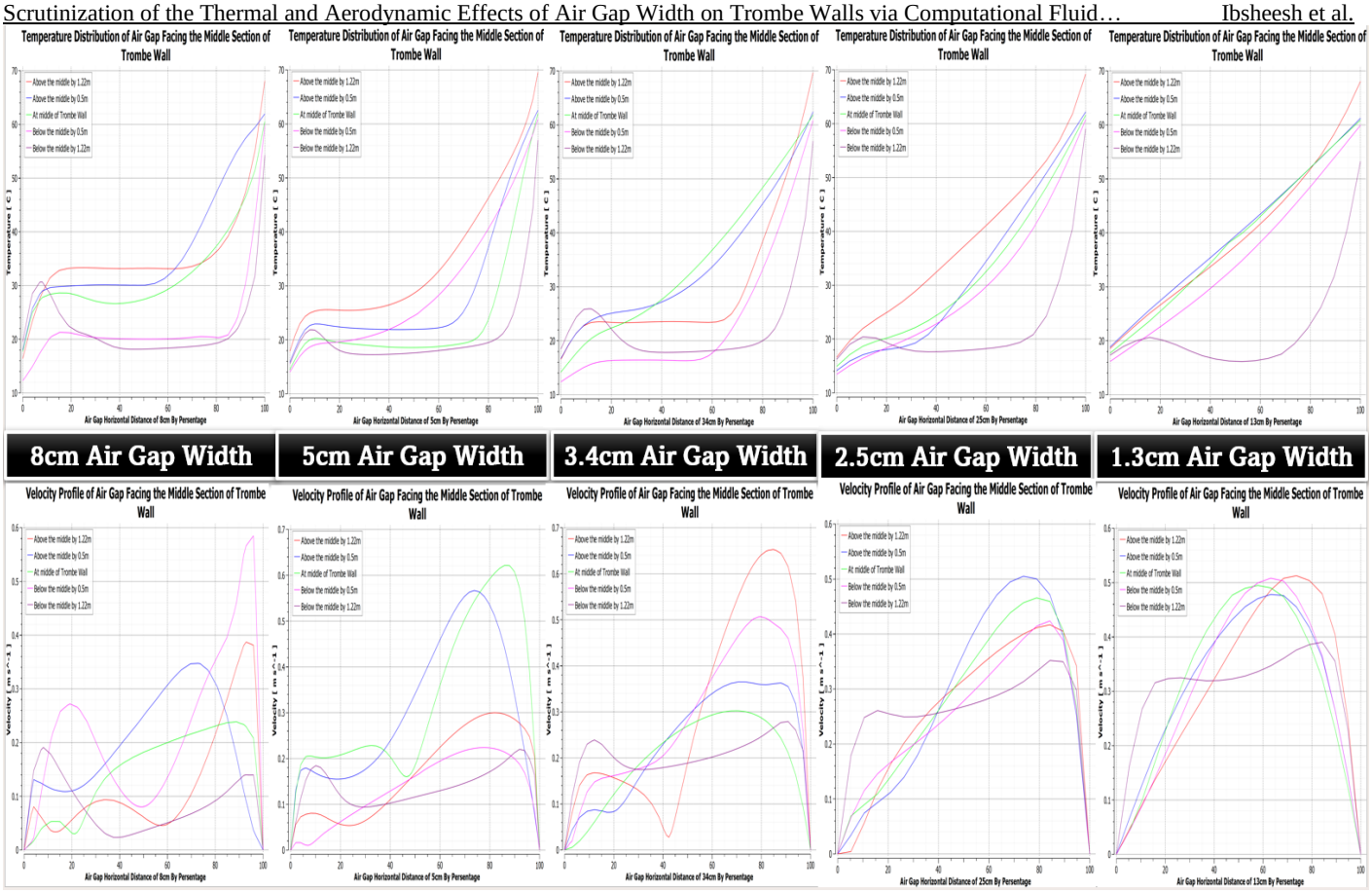

Appendix H. *Figure 5. Temperature distributions and Velocity at Middle Section of Air Gap*

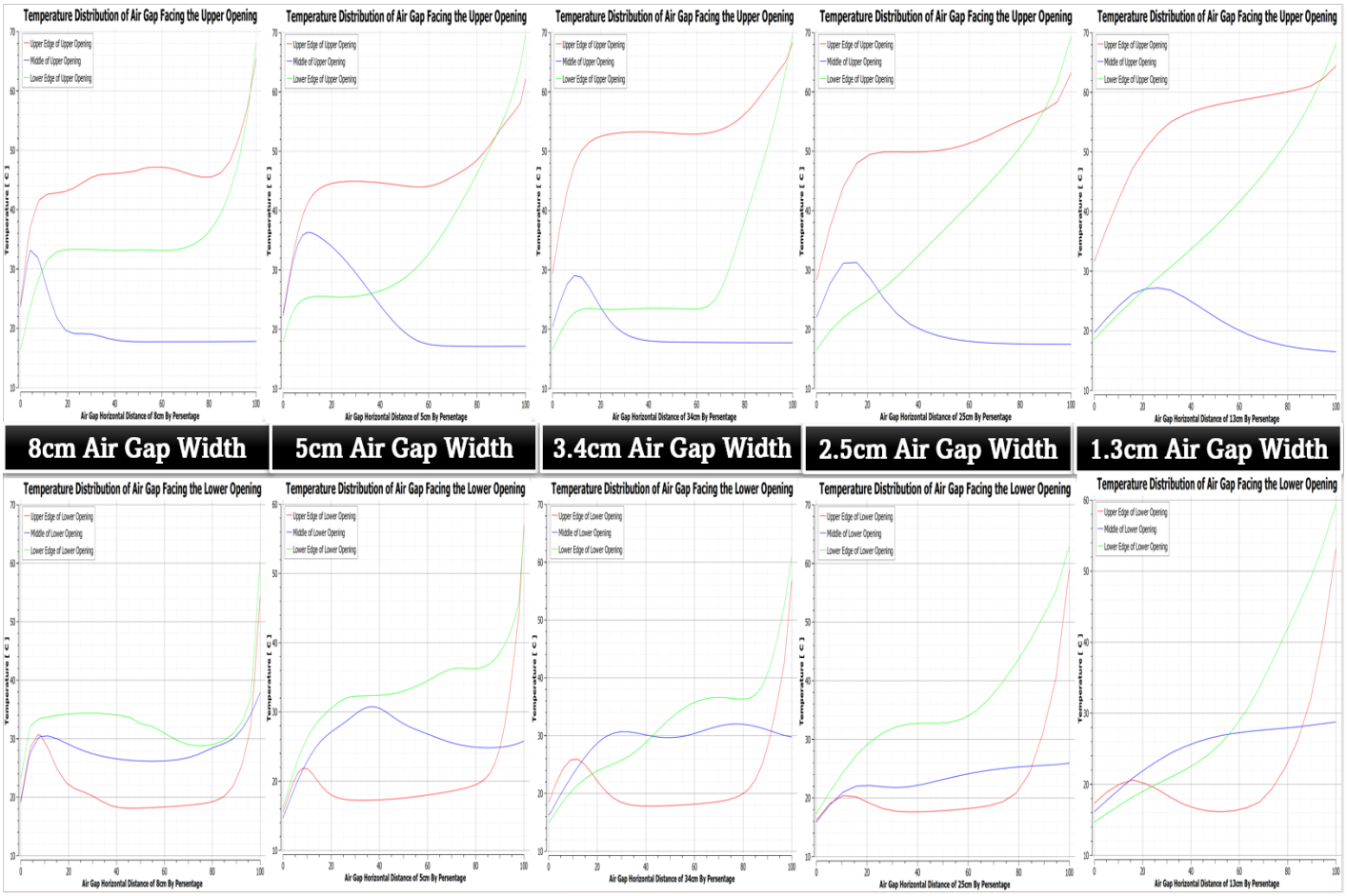

Appendix I. *Figure 6. Temperature distributions at Upper and Lower Opening of Air Gap*

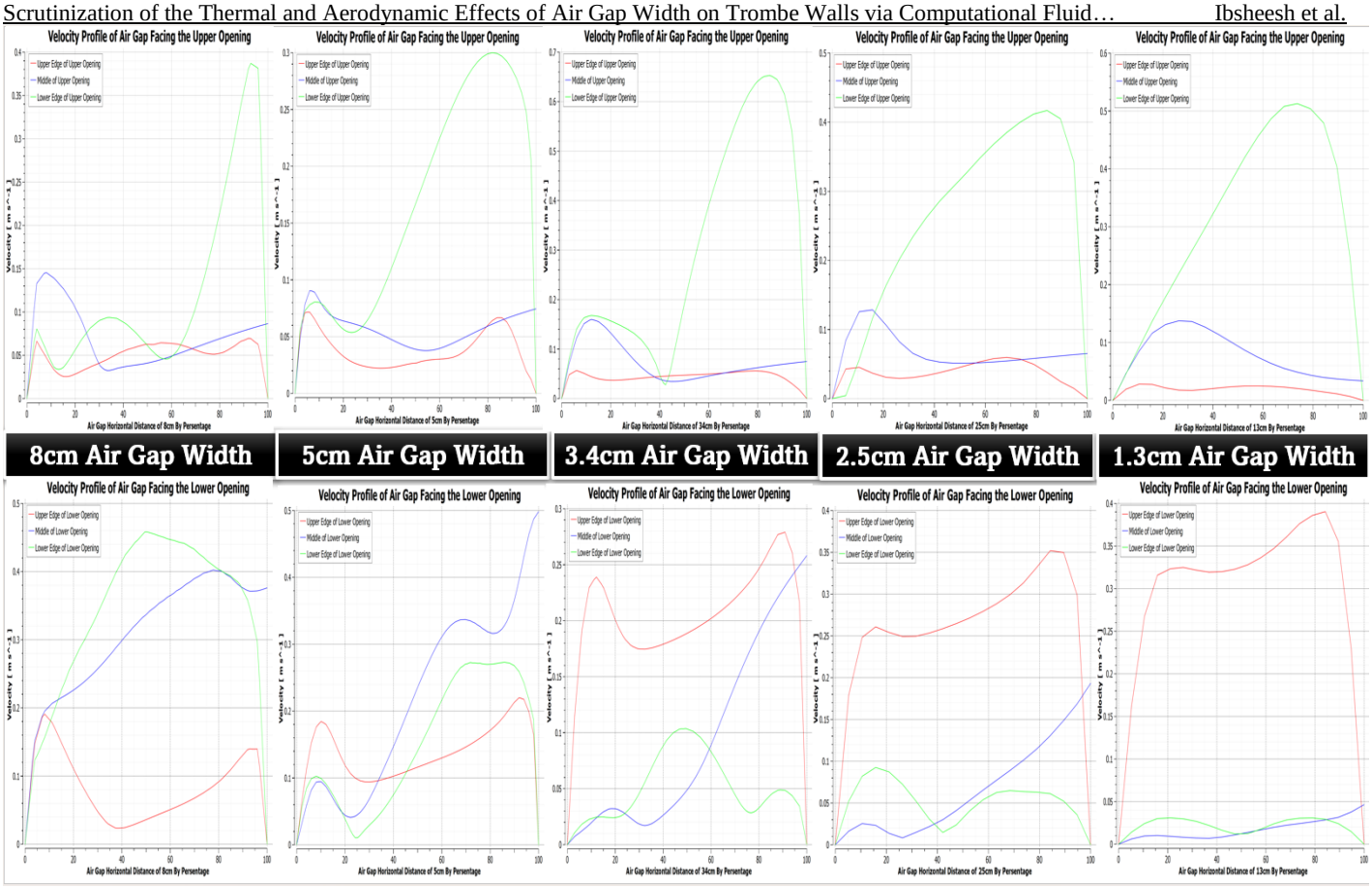

Appendix J. *Figure 7. Velocity Profile at Upper and Lower Opening of Air Gap*

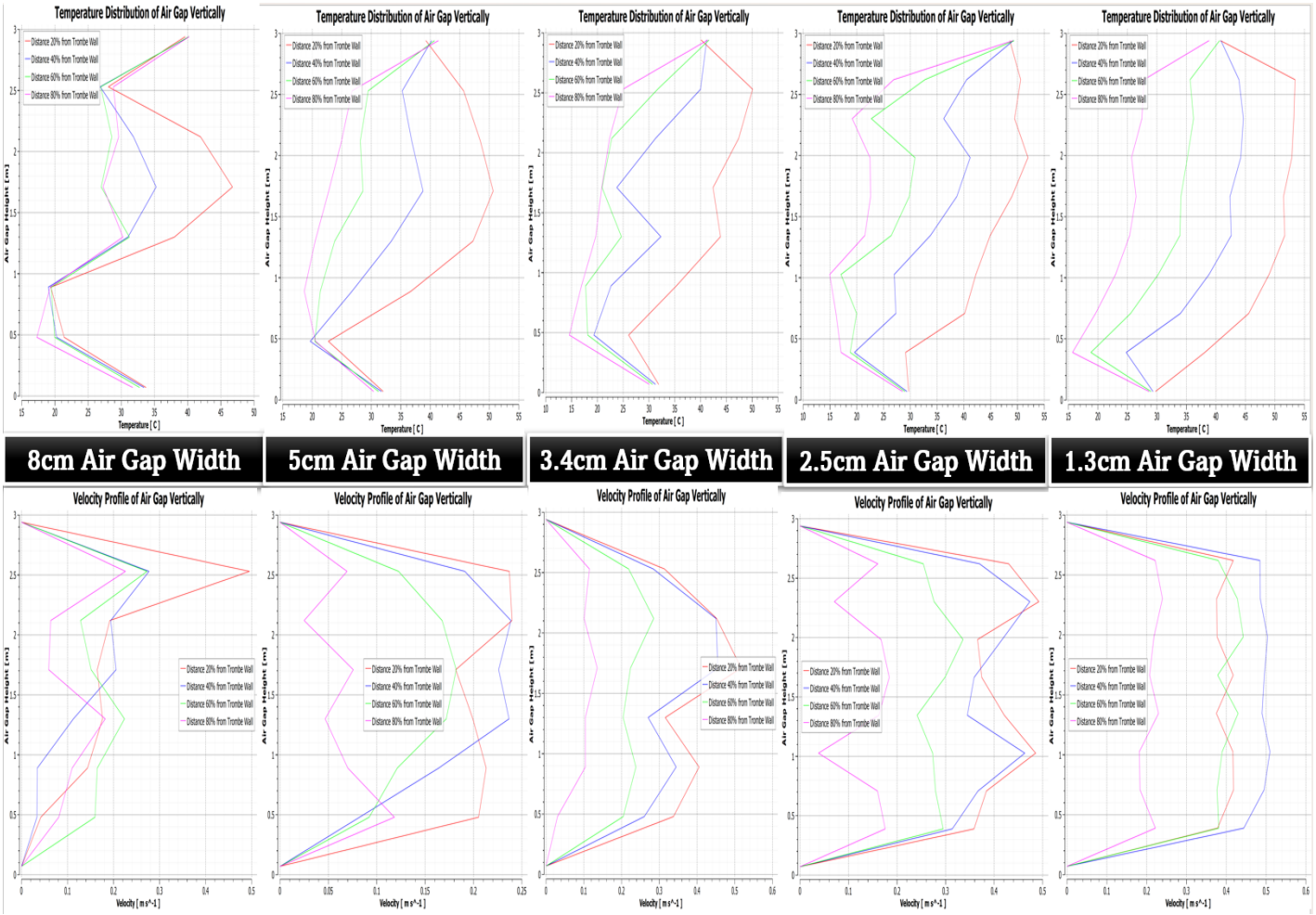

Appendix K. *Figure 8. Temperature and Velocity along the Air gap*

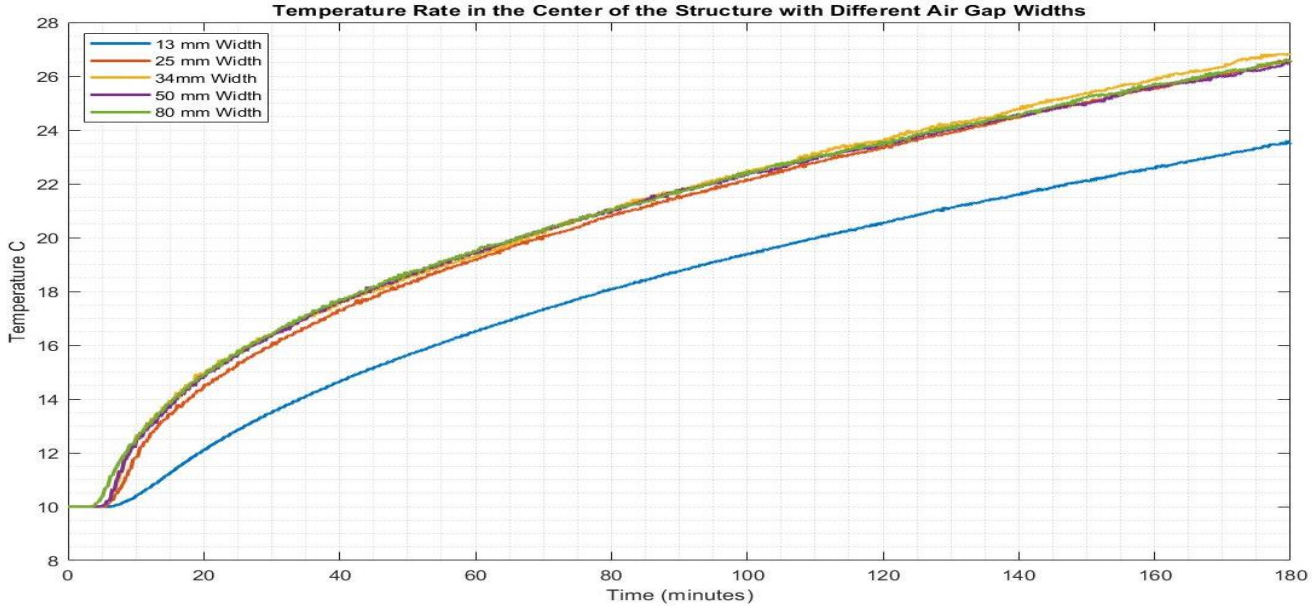

Appendix L. *Figure 9. Temperature VS Time*

Likewise, the $\mathbf{1.3}\ \boldsymbol{cm}$ width velocity profile exhibits a peak velocity at approximately **30**% of the width from the mass wall. Nevertheless, this velocity decreases as the air gap enlarges. For an $\mathbf{8}\boldsymbol{cm}$ width, two velocity peaks are perceived, creating a region around **55**% of the distance with lower air velocity relative to the air near the glass and the wall, where it enlarges as the air gap widens. Interestingly, the $\mathbf{5}\boldsymbol{cm}$ air gap width indicates the lowest temperature among all air gap widths but shows the highest air velocity. This observation implies the probability of an optimal air velocity existence at a $\mathbf{5}\boldsymbol{cm}$ air gap width or near that width. The decline in temperature can be explained by the high air velocity, leading to less time for the air to warm up.

Finally, figure **11** depicts the temperature variation over time at a point in the center of the structure of height $\mathbf{1.45}\ \boldsymbol{m}$. The findings features that the air gap of $\mathbf{8}\ \boldsymbol{cm}$ and $\mathbf{3.4}\ \boldsymbol{cm}$ facilitate faster heating of the structure compared to other widths, noting the 8cm width is more optimal than the $\mathbf{3.4}\ \boldsymbol{cm}$ width. Contrarily, the air gap of 5cm requires more time to heat up the structure, signifying that it is more effective for cooling than heating.

CONCLUSION

The study utilized a CFD simulation by Ansys to achieve fundamental insights into temperature distribution and air dynamics of air gaps within TW systems. The results conclude that an $\mathbf{8}\ \boldsymbol{cm}$ air gap width facilitates faster heating of the structure than other widths. However, the $\mathbf{5}\ \boldsymbol{cm}$ width indicates the slowest heating rate of all trial widths but has more air velocity, suggesting excellent cooling performance comparable to heating. Moreover, a wide air gap creates a region in the middle of the air gap that has a lower air velocity than the air close to the wall and glass, potentially leading to the formation of minor vortices. Suggestions for further investigation on air gap widths specifically around $\mathbf{5}\ \boldsymbol{cm}$ air gap width are recommended, as well as studying air gap widths with wide intervals for a better understanding of the drastic variation in the temperature and velocity, mainly in winter and summer scenarios.

REFERENCES

[1]- E. Morse, “Warming and Ventilating Apartments by Sun’s Rays”, US Patent No. 246,626, 1881.

[2]- J. Duffie and W. Beckman, “Solar Engineering of Thermal Processes”, John Wiley and Sons, Inc. 2013.

[3]- V. Aisya and J. Hendrarsakti, “Computational and Analytical Study of Trombe Wall Configurations within Bandung Weather Condition”, International Conference On Thermal Science And Technology, vol. 1984, 020019, 2018.

[4]- Ehsan F. Abbas, “Effect of Air Gap Width on the Evaluation of the Trombe Wall Efficiency”, International Review of Mechanical Engineering, vol. 13, no. 11, pp. 655–661, 2019.

[5]- S. S. Faris, M. T. Chaichan, M. F. Sachit, and J. M. Jaleel, “Simulation and Numerical Investigation of The Effect of Air Gap Thickness on Trombe Wall System”, International Journal of Application or Innovation in Engineering & Management, vol. 3, no. 11, pp. 159–168, 2014.

[6]- ANSYS, “ANSYS, Inc”, 23 1 2009. [Online]:https://www.afs.enea.it/project/neptunius/docs/fluent/html/th/main_pre.htm